ARTICLES

Syntheses, Structures, and Photoisomerization of (*E*)- and (*Z*)-2-*tert*-Butyl-9-(2,2,2-triphenylethylidene)fluorene

James W. Barr, Thomas W. Bell,* Vincent J. Catalano, Joseph I. Cline,* Daniel J. Phillips, and Rolando Procupez

Department of Chemistry, University of Nevada, Reno, Nevada 89557-0020

Received: August 4, 2005; In Final Form: October 11, 2005

"Sterically geared" 9-(2,2,2-triphenylethylidene)fluorene (**1**) is of potential interest as a photoactive moiety in molecular devices, and the 2-*tert*-butyl derivative (**6**) has been synthesized to investigate photoisomerization. *E* and *Z* stereoisomers of **6** were separated and identified by X-ray crystallography. The *tert*-butyl group does not introduce additional strain, and its close proximity to the trityl group in the *Z* isomer suggests an attractive van der Waals interaction. The UV spectra of (*E*)-**6** and (*Z*)-**6** are nearly identical, showing absorption bands that are similar to those of fluorene occurring at wavelengths longer than 240 nm. Photoisomerization of **6** was investigated at 266, 280 and 320 nm. Solutions initially containing only (*E*)-**6** or (*Z*)-**6** were irradiated with pulsed laser light, monitoring isomerization by ^{1}H NMR spectroscopy. Negligible photodecomposition was observed when the solutions were agitated by N_2 ebullition. Experimental data were fitted to theoretical curves to obtain photoisomerization quantum yields (ϕ_{ZE} and ϕ_{EZ}) ranging from 0.04 to 0.09. This first photoisomerization study of a dibenzofulvene reveals significant quantum yields, despite theoretical prediction of inefficient or negligible isomerization of the parent hydrocarbon, fulvene. Thermal isomerization of **6** at 270 °C ($t_{1/2}$ = 120 min) was also followed by ^{1}H NMR spectroscopy, resulting in an estimated activation energy ($\Delta G^{\ddagger}$) of 43 kcal/mol.

1. Introduction

Steric gearing[1] between the triphenylmethane and planar fluorene moieties of 9-(2,2,2-triphenylethylidenefluorene) (**1**, see Chart 1) produces significant in-plane distortion of the exocyclic C═C double bond.[2] There is intense current interest in molecular devices,[3] such as switches[4] and motors,[5] and we postulate that light-activated rotation about this double bond could produce rotary motion of the triphenylmethane "propeller" in a suitable derivative of **1**. This double bond linking the fluorene and triphenylmethane components of **1** is part of a dibenzofulvene (also called 9-methylenefluorene) chromophore (**2**, see Chart 1), which may be considered a fused-ring 1,1-diarylethylene. While photoisomerization of 1,2-diarylethylenes (e.g., *trans*- and *cis*-stilbenes) has been studied extensively,[6] the photochemistry of 1,1-diarylethylenes has been less well investigated. Thermal barriers for rotation about the exocyclic double bond of fulvene have been theoretically modeled[7] and experimentally determined in the case of substituted fulvenes.[8] Excited-state calculations suggest that fulvenes can photoisomerize,[9] but this has not yet been shown experimentally. Thermal isomerization of 2-nitro- and 2-bromo-9-(4-nitrobenzylidene)fluorene was reported more than five decades ago.[10] Reported herein is the first known case of photoisomerization of a dibenzofulvene and possibly even of any fulvene or 1,1-diarylethene.

CHART 1

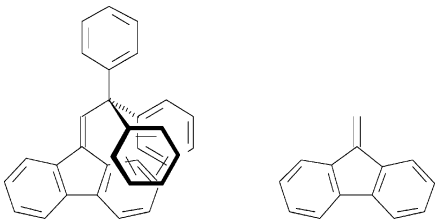

1 **2**

2. Synthesis

2.1. Synthetic Overview. (*E*)- and (*Z*)-2-*tert*-butyl-9-(2,2,2-triphenylethylidene)fluorene (**6**) were prepared by the method developed previously for the synthesis of 9-(2,2,2-triphenylethylidene)fluorene (**1**).[2] As shown in Scheme 1, 2-*tert*-butylfluorene (**3**) was converted by air oxidation to 2-*tert*-butylfluorenone (**4**).[11] As reported for fluorenone,[12] Wittig reaction of **4** with bromomethylenetriphenylphosphorane gave the bromomethylene derivative **5**, in this case as a ca. 1:1 mixture of *E* and *Z* stereoisomers. Reaction of (*E*/*Z*)-**5** with triphenylmethyllithium then afforded a 1:1 mixture of (*E*)-**6** and (*Z*)-**6**, in significantly higher yield than reported for the unsubstituted analogue (**1**).[2] These target stereoisomers were separated by sequential column chromatography on alumina and crystallization from hexane. Analytically pure samples of both (*E*)-**6** and (*Z*)-**6** were obtained for photoisomerization studies.

2.2. (*E*/*Z*)-2-*tert*-Butyl-9-bromomethylenefluorene (5). A suspension of bromomethyltriphenylphosphonium bromide (4.06

* To whom correspondence should be addressed. E-mail: twb@unr.edu; cline@chem.unr.edu.

10.1021/jp054345l CCC: $30.25
Published on Web 12/01/2005

SCHEME 1:[a] **Synthesis of (*E*)- and (*Z*)-2-*tert*-Butyl-9-(2,2,2)-triphenylethylidenefluorene**

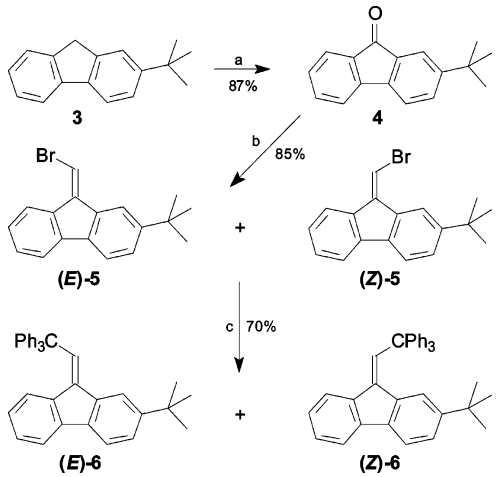

[a] (a) O_2, Triton B, pyridine, 25 °C, 36 h. (b) $BrCH_2PPh_3Br$, NaHMDS, THF, −60 °C; **4**, 25 °C, 18 h. (c) Ph_3CH, *n*BuLi, THF, 0 °C; **5**, −78−25 °C, 25 h. Triton B = benzyltrimethylammonium hydroxide; NaHMDS = sodium bis(trimethylsilyl)amide.

g, 9.31 mmol) in anhydrous THF (40 mL) was cooled to −60 °C under N_2, and a solution of 2 M sodium bis(trimethylsilyl)-amide in anhydrous THF (4.6 mL, 9.2 mmol) was added dropwise. The resulting yellow suspension was stirred for 40 min, and a solution of 2-*tert*-butyl-9*H*-fluorenone[11] in anhydrous THF (2.01 g, 8.53 mmol) was added. The reaction mixture was then allowed to warm gradually to room temperature and stirred for 18 h. Water was added (50 mL), and the resulting mixture was extracted with diethyl ether (3 × 25 mL). The combined ether solutions were dried over anhydrous Na_2SO_4 and then concentrated to dryness by rotary evaporation. The residue was dried under vacuum, giving 4.50 g of a deep red/brown oil. Column chromatography on silica gel (32−60 μm), eluting with hexane, gave 2.27 g of a 1:1 mixture of (*E*)- and (*Z*)-**5** (85%) as an orange gum-like solid. ^{1}H NMR (300 MHz, $CDCl_3$): δ 8.56 (d, J = 1.5 Hz, 1 H), 8.52 (d, J = 7.7 Hz, 1 H), 7.2−7.8 (m, 14 H), 1.42 (s, 9 H, *t*Bu), 1.38 (s, 9 H, *t*Bu).

2.3. (*E*)- and (*Z*)-2-*tert*-Butyl-9-(2,2,2-triphenylethylidene)-fluorene (6). A solution of triphenylmethane (3.09 g, 12.6 mmol) in anhydrous THF (15 mL) was cooled to −78 °C under N_2, and a solution of *n*-butyllithium in hexane (1.58 M, 6.5 mL) was added, producing a pink solution. The solution was stirred at 0 °C for 40 min, and then the resulting blood-red solution of the trityl anion was recooled to −78 °C and a solution of (*E*/*Z*)-2-*tert*-butyl-9-bromomethylenefluorene (2.47 g, 7.90 mmol) in 10 mL of anhydrous THF was added. The reaction mixture was allowed to warm gradually to room temperature and stirred for 25 h. Water (75 mL) was added, and the resulting mixture was extracted with diethyl ether (4 × 25 mL). The combined ether solutions were dried over anhydrous Na_2SO_4 and then concentrated to dryness by rotary evaporation. The residue was dried under vacuum, giving 5.03 g of a yellow oil, consisting primarily of (*Z*)-**6** (R_f 0.16 alumina, hexane), (*E*)-**6** (R_f 0.19, alumina, hexane), and triphenylmethane (R_f 0.34, alumina, hexane). Sequential column chromatography (50 g of 80−200 mesh alumina, hexane) and fractional crystallization from hexane gave a total of 2.63 g (70%) of the products (0.59 g of pure (*Z*)-**6**, 0.35 g of pure (*E*)-**6**, and the reminder as mixed fractions).

(*Z*)-**6:** mp 221−223 °C; ^{1}H NMR (300 MHz, CD_2Cl_2): δ = 7.84 (s, 1 H), 7.77 (d, J = 7.33 Hz, 1 H), 7.7 (d, J = 7.32 Hz, 1 H), 7.56 (d, J = 8.06 Hz, 1 H), 7.24−7.33 (m, 18 H), 6.84 (s, 1 H), 0.93 (s, 9 H; *t*Bu); ^{13}C NMR (75 MHz, CD_2Cl_2): δ = 150.0, 141.5, 140.0, 139.2, 138.8, 135.8, 130.8, 128.8, 126.9, 126.2, 120.4, 119.6, 118.8, 62.1, 35.5, 31.9; IR (KBr): ν = 3052 (m), 2963 (m), 1594 (m), 1488 (s), 1444 (s), 1420 (w), 1262 (m), 1035 (w), 823 (s), 765 (w), 748 (m), 730 (s), 701 (s) cm^{-1}; MS (EI) *m*/*z* (%) 477 (5.2) [M^+ + 1], 476 (12.7) [M^+], 419 (9.4), 341 (36.3), 265 (11.4), 252 (8.7), 165 (59.1), 139 (13.9), 57 (100); UV/Vis (0.0092 mM, CH_3CN): λ_{max} (ϵ) = 236 (34076), 254 (28261), 262 (35870), 288 (14130), 305 (13772), 318 (13261) nm; elemental analysis calcd (%) for $C_{37}H_{32}$: C 93.36; H 6.78; found: C 93.12, H 6.70.

(*E*)-**6:** mp 215−217 °C; ^{1}H NMR (300 MHz, CD_2Cl_2): δ = 7.81 (s, 1 H), 7.76 (s, 1 H), 7.60 (t, J = 7.58 Hz, 1 H), 7.41 (dd, J = 8.06 Hz, 1 H), 7.22−7.30 (m, 16 H), 7.13 (t, J = 7.32 Hz, 1 H), 6.63 (t, J = 7.59 Hz, 1 H), 6.45 (d, J = 8.05 Hz, 1 H), 1.38 (s, 9 H, *t*Bu); ^{13}C NMR (75 MHz, CD_2Cl_2): δ = 50.4, 146.8, 138.4, 138.0, 136.0, 135.2, 130.0, 127.6, 126.4, 125.0, 118.4, 116.4, 62.1, 35.5, 31.9; IR (KBr): ν = 3056 (m), 2955 (m), 1596 (m), 1488 (s), 1445 (s), 1421 (w), 1262 (m), 1034 (w), 835 (s), 769 (w), 752 (m), 730 (s), 700 (s) cm^{-1}; MS (EI) *m*/*z* (%) 476 (6.9) [M^+], 419 (5.3), 341 (20.0), 265 (7.0), 252 (5.7), 165 (39.0), 139 (9.8), 57 (100); UV/Vis (0.0092 mM, CH_3CN): λ_{max} (ϵ) = 235 (38456), 255 (33913), 263 (43478), 287 (18152), 305 (15978), 317 (14022) nm; elemental analysis calcd (%) for $C_{37}H_{32}$: C 93.36; H 6.78; found: C 93.09, H 6.73.

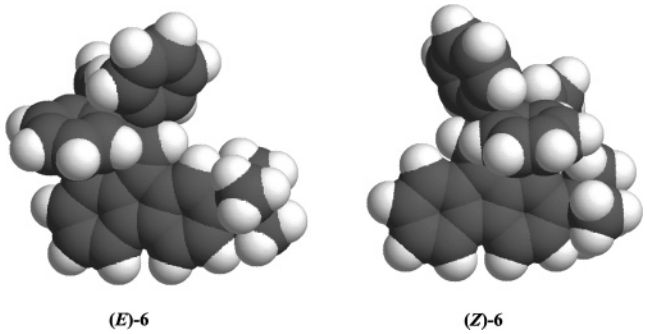

Figure 1. Space-filling diagrams of crystallographically determined structures of (*E*)- and (*Z*)-2-*tert*-butyl-9-(2,2,2)-triphenylethylidene-fluorene (**6**).

3. Structures of (*E*)-6 and (*Z*)-6

The structures of both (*E*)-**6** and (*Z*)-**6** were determined by single-crystal X-ray diffraction. In both structures, there are two molecules in the asymmetric unit, and each *tert*-butyl group is rotationally disordered. Simple models of this disorder provided satisfactory refinements. A space-filling diagram of a representative conformation of each stereoisomer is shown in Figure 1. It is apparent from the diagram of (*E*)-**6** (Figure 1, left) that there is no steric interference between the triphenylmethyl (trityl) and *tert*-butyl groups. For the corresponding *Z* isomer (Figure 1, right), the closest C−C distance between phenyl and methyl carbons is ca. 3.86 Å for either molecule in the asymmetric unit.

The parent hydrocarbon lacking a *tert*-butyl group (**1**) shows an unusual distribution of bond strain. Most of the distortion around the exocyclic double bond in this overcrowded trisubstituted alkene occurs as bond angle deformation, rather than torsional strain. Table 1 compares the bond angles for the exocyclic double bonds of (*E*)- and (*Z*)-**6** with those of **1**. It is clear from this comparison that the geometries of this key, photoactive double bond are essentially the same in all three compounds and that the *tert*-butyl group does not introduce

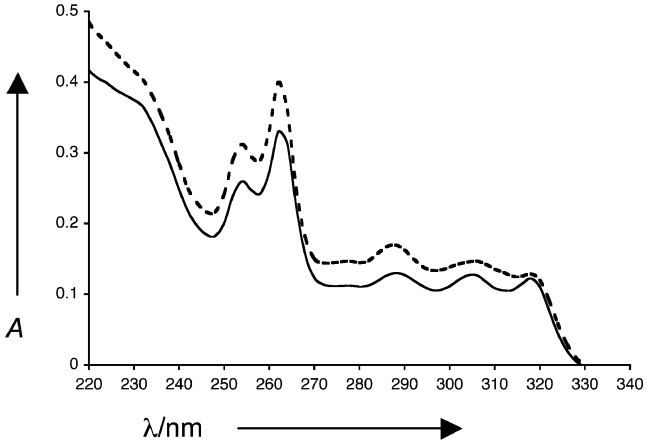

Figure 2. UV absorption spectra of both stereoisomers of 2-*tert*-butyl-9-(2,2,2)-triphenylethylidenefluorene (CH_3CN, 9.2 μM): (*E*)-**6**, dashed line; (*Z*)-**6**, solid line.

TABLE 1: Crystallographically Determined Bond Angles (deg) for the Exocyclic Double Bond of (*E*)-6, (*Z*)-6, and 1[2]

(*E*)-**6**: R^1 = *t*Bu, R^2 = H
(*Z*)-**6**: R^1 = H, R^2 = *t*Bu
1: $R^1 = R^2$ = H

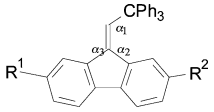

alkene	α_1	α_2	α_3
(*E*)-**6** (mol 1)	133.2(5)	133.7(5)	121.8(5)
(*E*)-**6** (mol 2)	133.6(5)	134.8(5)	120.8(5)
(*Z*)-**6**(mol 1)	134.1(4)	133.7(4)	121.7(4)
(*Z*)-**6** (mol 2)	130.8(3)	132.6(3)	122.5(3)
1 (mol 1)	134.7(3)	134.5(3)	120.8(3)
1 (mol 2)	133.5(3)	134.3(3)	121.1(3)

additional strain in **6**. Both stereoisomers of **6** show the same degree of "steric gearing" as observed previously for **1**.[2] Moreover, in (*Z*)-**6**, close proximity between the trityl and *tert*-butyl groups may result in a van der Waals interaction that is attractive.

Crystallographic Data. Crystal data for (*E*)-**6**: $a = 12.221(1)$, $b = 17.921(2)$, $c = 13.524(3)$ Å, $\alpha = 90°$, $\beta = 107.82(1)°$, $\gamma = 90°$, $V = 2820$ Å^3, $M_r = 476.66$, $P2(1)$, $Z = 2$, ρ_{calcd} 1.123 g cm^{-3}, 6296 independent reflections. Crystal data for (*Z*)-**6**: $a = 11.272(3)$, $b = 14.504(3)$, $c = 17.102(3)$ Å, $\alpha = 84.54(2)°$, $\beta = 86.25(2)°$, $\gamma = 81.33(2)°$, $V = 2748$ Å^3, $M_r = 476.66$, P-1, ρ_{calcd} 1.152 gcm^{-3}, 8506 independent reflections. Suitable crystals were coated in epoxy cement and mounted on a Siemens P4 diffractometer. Data were collected at room temperature, and both structures were solved by direct methods. The non-hydrogen atoms were refined with anisotropic thermal parameters. Hydrogen atom positions were calculated using a riding model with a C−H distance fixed at 0.96 Å and a thermal parameter 1.2 times the host carbon atom. The structures were refined on F^2 by a full-matrix least-squares program using SHELXTL97.[15] The occupancies of the positionally disordered *tert*-butyl groups in (*E*)-**6** refined to 69 and 31% and to 75 and 25% while in (*Z*)-**6** they refined to 89 and 11% and to 57 and 43%. Final *R* values were for (*E*)-**6**, $R1 = 0.0599$, $wR2 = 0.1463$ for 5478 data, and for (*Z*)-**6**, $R1 = 0.0608$, $wR2 = 0.1065$ for 7188 data, both with $I > 2\sigma(I)$. Supplementary crystallographic data consisting of positional parameters, bond lengths and angles, hydrogen atom positions, and thermal parameters are given in the Supporting Information.

4. Spectroscopy and Photoisomerization Dynamics

4.1. Absorption Spectroscopy. Figure 2 shows the UV absorption spectra of (*E*)-**6** and (*Z*)-**6**, which do not absorb visible light. These spectra are nearly identical, confirming that interaction between the *tert*-butyl and trityl groups only has a minor influence on the structure of **6**. We have not assigned the electronic spectrum of **6**, but we note that the band structure is similar to that of fluorene at wavelengths longer than 240 nm.

4.2. Photoisomerization Measurements. Photoisomerization quantum yields of **6** were measured at 266, 280, and 320 nm, corresponding to the approximate locations of absorption maxima shown in Figure 2. The photoisomerization was studied at room temperature in vigorously agitated perdeuterioacetonitrile solutions saturated with N_2. Sample solutions initially contained only (*E*)-**6** or (*Z*)-**6** and the progress of the photoisomerization was monitored by alternately irradiating the sample with UV light from a pulsed laser source and then measuring the ^{1}H NMR spectrum. The relative amounts of the *Z* and *E* isomers were obtained from the peak heights of the *tert*-butyl protons, located at 0.93 and 1.38 ppm for the *Z* and *E* isomers, respectively.

The light source for the photoisomerization experiments was the fourth harmonic (266 nm) of a 5 ns pulse, 10 Hz repetition rate Nd:YAG laser or a frequency-doubled dye laser pumped by the second harmonic of the Nd:YAG laser (for 280 and 320 nm experiments). The average laser pulse energy was typically 2.0 mJ. The photoisomerization measurements were performed in a flat-bottomed, 1 cm diameter, fused silica NMR tube. The UV laser light was directed through the bottom of the tube. The sample solution volume was typically 3.2 mL with a 5.0×10^{-4} M concentration of molecule **6**. This gives an optical path length of about 4 cm and a very high optical density at the wavelengths in this experiment, so that the entire laser pulse is absorbed by the sample solution. During laser irradiation, a stream of N_2 presaturated with the perdeuterioacetonitrile solvent was introduced near the bottom of the sample tube using a stainless steel syringe needle inserted through a septum at the top of the tube. The flow of N_2 served to both displace dissolved O_2 and to vigorously agitate the solution during irradiation. Vigorous agitation is necessary to ensure that all molecules have an equal opportunity to absorb a photon over the course of an irradiation cycle (typically 15−60 s).

4.3. Data Analysis and Results. The average number of photons, *x*, absorbed per molecule after an irradiation time, *t*, is obtained from the number of photons delivered to the sample divided by the number of absorbing molecules in the sample:

$$x(t) = \left(\frac{\nu_l E_l \lambda_l t}{hc}\right)\left(\frac{1}{CVN_A}\right) \qquad (1)$$

In eq 1, λ_l, E_l, and ν_l are the laser wavelength, pulse energy, and pulse repetition rate; *C* and *V* are the sample solution molarity and volume; and *h*, *c*, and N_A are Planck's constant, the speed of light, and Avogadro's number, respectively. For a typical 5.0×10^{-4} M, 3.2 mL sample solution, irradiation by 2.0 mJ pulses of 280 nm light at 10 Hz results in an average absorption rate of 0.028 photons/molecule·s.

The mole fraction (f_E or f_Z) for each isomer was obtained from the ^{1}H NMR spectra by dividing its *tert*-butyl ^{1}H NMR peak height by the sum of the *tert*-butyl ^{1}H NMR peak heights for the two isomers. Under the experimental conditions described above and in Section 4.1, negligible photodecomposition of (*E*)-**6** or (*Z*)-**6** was observed in the NMR spectra for total

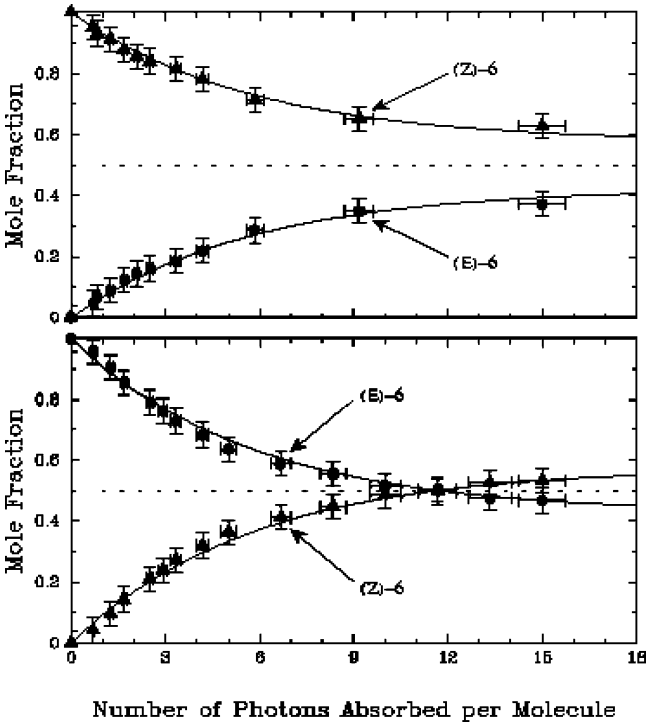

Figure 3. Photoisomerization data at 266 nm showing mole fractions of (Z)-**6** (▲ symbols) and (*E*)-**6** (● symbols) as a function of the average number of photons absorbed. The upper panel shows data for $[Z]_0 = 1$. The lower panel shows data for $[E]_0 = 1$. Solid curves show a fit to the kinetic model with photoisomerization rates $\phi_{ZE} = 0.074$ and $\phi_{EZ} = 0.10$ in eqs 2 and 3.

irradiations of at least 80 photons/molecule, so that $f_E + f_Z = 1$, independent of the number of photons, x. In the absence of solution agitation during irradiation by means of N_2 ebullition, photodecomposition was demonstrated by the growth of new features in the NMR spectra and by a yellow discoloration of the solution. Significantly higher laser pulse energies in the absence of solution agitation during irradiation resulted in a black precipitate.

Figure 3 shows the mole fraction of (*E*)-**6** and (*Z*)-**6** as a function of the average number of absorbed photons in a 266 nm photoisomerization experiment. The upper panel shows data for an initial solution containing only the *Z* isomer and the lower panel shows data starting with the *E* isomer. The photostationary state at $x \rightarrow \infty$ shows a $[Z]/[E]$ ratio of 1.4. Because photodecomposition is negligible over the duration of our experiments, we assume reversible photoisomerization:

$$Z + h\nu \xrightarrow{\phi_{ZE}} E \tag{2}$$

$$\mathrm{E} + h\nu \xrightarrow{\phi_{EZ}} \mathrm{Z} \tag{3}$$

where ϕ_{ZE} (λ) and ϕ_{EZ} (λ) indicate the wavelength-dependent photoisomerization quantum yields for the processes in eqs 2 and 3. At a given wavelength, the ratio of the forward and reverse quantum yields can be obtained from the photostationary state population ratio and the ratio of the measured molar absorptivities of the *E* and *Z* isomers, $\in_E$ (λ) and $\in_Z$ (λ):

$$\frac{\phi_{ZE}}{\phi_{EZ}} = \left(\frac{[E](x=\infty)}{[Z](x=\infty)}\right)\left(\frac{\in_E}{\in_Z}\right) \tag{4}$$

To obtain absolute photoisomerization quantum yields, we quantitatively modeled measurements of the type shown in Figure 3. The kinetic analysis is complicated by the slightly different molar absorptivities of the *E* and *Z* isomers. The change in mole fraction per average number of absorbed photons/molecule is given by

$$\frac{\mathrm{d}f_E}{\mathrm{d}x} = \frac{\phi_{ZE}(1-f_E)\in_Z - \phi_{EZ}f_E \in_E}{(1-f_E)\in_Z + f_E \in_E} = -\frac{\mathrm{d}f_Z}{\mathrm{d}x} \tag{5}$$

Equation 5 can be integrated numerically for a choice of the $f_E(x = 0)$ initial condition, quantum yields, and molar absorptivities.

The curves in Figure 3 show fits to the experimental data obtained by nonlinear least squares optimization of ϕ_{ZE} and ϕ_{EZ} in a numerical integration of eq 5. Table 2 shows average photoisomerization quantum yields obtained in this way from multiple measurements at each of the three photoisomerization wavelengths studied as well as the $[Z]/[E]$ ratio in the photostationary state. Quantum yields range from 4 to 9% and the *Z* isomer predominates in the photostationary state at each wavelength examined.

TABLE 2: Wavelength-Dependent Quantum Yields for Photoisomerization of 6 in Acetonitrile-d_3

λ, nm	ϕ_{ZE}	ϕ_{EZ}	$([Z]/[E])_{ps}$[a]
266	0.08	0.09	57/43
280	0.04	0.04	53/47
320	0.07	0.09	58/42

[a] Photostationary state.

5. Discussion

The fulvene S_1 excited-state dynamics calculations of Bearpark et al.[9b] predict a very low photoisomerization quantum yield which would only be measurable at the 0−0 vibrational origin. In contrast, the dibenzofulvene chromophore of **6** shows significant photoisomerization at both 320 nm (presumably near the S_1 origin) and 280 nm (vibrationally excited S_1). The lower quantum yield at 280 nm may indicate that vibrational excitation inhibits photoisomerization, as is predicted for fulvene. At 266 nm (presumably excitation to a higher lying electronic state) the quantum yield is similar to that at 320 nm.

The measured photoisomerization quantum yields in Table 2 are somewhat smaller than those measured for the well-known and widely studied cis−trans isomerization of stilbene, which are typically around 0.5 for $\phi_t \rightarrow c$ and 0.3 for $\phi_c \rightarrow t$.[6d] Perhaps due to the higher symmetry of the substituted dibenzofulvene rotor of **6**, its "forward" and "reverse" quantum yields are more equitable than is seen in stilbene. To investigate the origin of the slight difference in the quantum yields, we examined the position of the thermodynamic equilibrium between the two isomers of **6**.

A study of the isomerization equilibrium at room temperature was attempted by catalysis using photolytically generated iodine radicals, as reported previously for stilbene.[14] Solutions of pure (*Z*)-**6** and iodine in CD_3CN or toluene-d_8 were irradiated at 532 nm. No (*E*)-**6** was observed, but decomposition occurred after prolonged irradiation. On the other hand, we found that prolonged heating of liquid (*Z*)-**6** (mp 221−223 °C) at 270 °C gave a 65/35 equilibrium ratio for [*Z*]/[E], and the same equilibrium ratio was observed for fast thermal isomerization at 360 °C. This equilibrium ratio gives a $\Delta G°$ for $E \rightarrow Z$ of −0.7 kcal/mol, which suggests that weak van der Waals attractions between the *tert*-butyl and trityl substituents slightly stabilize the *Z* isomer. This C═C torsional potential asymmetry, along with dynamical hysteresis effects due to coupling of

solvent motions to the photoisomerization dynamics, could be responsible for the slightly larger $E \rightarrow Z$ quantum yield relative to that for $Z \rightarrow E$.

From the half-life of the isomerization at 270 °C (120 min) an activation free energy ($\Delta G^{\ddagger}$) of 43 kcal/mol was estimated. This result shows that the π bond of the exocyclic C═C group of **6** is much stronger than that of (*Z*)-2-bromo-9-(*p*-nitrobenzylidene)fluorene, which isomerizes upon melting at 154 °C.[10b] The C═C torsional barrier for **6** is only slightly smaller than that calculated for fulvene (45.6 kcal/mol),[7] which has not been measured experimentally. The torsional barrier for 6-dimethylaminofulvene was found to be 13.5 kcal/mol,[8a] again showing that conjugating substituents on the exocyclic C═C group weaken the π bond.

6. Conclusion

We report what is, to our knowledge, the first experimental demonstration of the photoisomerization of a substituted dibenzofulvene. The dibenzofulvene chromophore of this molecule serves as a photoenergized rotor that is mechanically geared into a trityl base, functioning as a prototype for light-driven molecular devices, such as switches and motors. Thermal stabilities of stereoisomers and significant photoisomerization quantum yields, ranging from 4 to 9%, indicate that rotor chromophores based on dibenzofulvene show promise for such applications.

Acknowledgment. Financial support for this research was provided by the National Science Foundation (Nanoscale Interdisciplinary Research Team project # 021059). We also thank Professors John H. Frederick, Michael G. B. Drew, and Christine R. Cremo for their intellectual contributions to this project.

Supporting Information Available: Tables of crystallographic information including atomic coordinates, bond lengths and angles, and thermal parameters for (*Z*)- and (*E*)-**6** are given in CIF format. Figures displaying thermal ellipsoids for both molecules in the asymmetric units of the crystals of (*Z*)- and (*E*)-**6** are also shown.

References and Notes

(1) Hennrich, G.; Anslyn, E. V. *Chem. Eur. J.* **2002**, *8*, 2219−2224.

(2) Bell, T. W.; Catalano, V. J.; Drew, M. G. B.; Phillips, D. J. *Chem. Eur. J.* **2002**, *8*, 5001−5006.

(3) (a) Balzani, V.; Credi, A.; Raymo, F. M.; Stoddart, J. F. *Angew. Chem., Int. Ed.* **2000**, *39*, 3348−3391. (b) Sauvage, J.-P., Ed. *Molecular Motors and Machines: Structure and Bonding*; Springer: Berlin, 2001; Vol. 99. (c) Tseng, H.-R.; Stoddart, J. F. In *Modern Arene Chemistry*; Astruc, D., Ed.; Wiley-VCH: Weinheim, 2002; pp 574−599. (d) Badjiæ, J. D.; Balzani, V.; Credi, A.; Silvi, S.; Stoddart, J. F. *Science (Wash., D.C.)* **2004**, *303*, 1845−1849. (e) Easton, C. J.; Lincoln, S. F.; Barr, L.; Onagi, H. *Chem. Eur. J.* **2004**, *10*, 3120−3128.

(4) (a) Huck, N. P. M.; Feringa, B. L. *J. Chem. Soc., Chem. Commun*. **1995**, 1095−1096. (b) Schoevaars, A. M.; Kruizinga, W.; Zijlstra, R. W. J.; Veldman, N.; Spek, A. L.; Feringa, B. L. *J. Org. Chem*. **1997**, *62*, 4943−4948. (c) Raymo, F. M.; Giordani, S. *Proc. Nat. Acad. Sci*. **2002**, *99*, 4941−4944. (d) Feringa, B. L.; van Delden, R. A.; Koumura, N.; Geertsema, E. M. *Chem. Rev*. **2000**, *100*, 1789−1816. (e) Raymo, F. M. *Adv. Mater*. **2002**, *14*, 401−414. (f) de Jong, J. J. D.; Lucas, L. N.; Hania, R.; Pugzlys, A.; Kellogg, R. M.; Feringa, B. L.; Duppen, K.; van Esch, J. H. *Eur. J. Org. Chem*. **2003**, 1887−1893. (g) Lehmann, J.; Camalet, S.; Kohler, S.; Hänggi, P. *Chem. Phys. Lett*. **2003**, *368*, 282−288.

(5) (a) Koumura, N.; Zijlstra, R. W. J.; van Delden, R. A.; Harada, N.; Feringa, B. L. *Nature* **1999**, *401*, 152−155. (b) Koumura, N.; Geertsema, E. M.; Meetsma, A.; Feringa, B. L. *J. Am. Chem. Soc*. **2000**, *122*, 12005−12006. (c) Geertsema, E. M.; Koumura, N.; ter Wiel, M. K. J.; Meetsma, A.; Feringa, B. L. *J. Chem. Soc., Chem. Commun*. **2002**, 2962−2963. (d) van Delden, R. A.; Koumura, N.; Harada, N.; Feringa, B. L. *Proc. Nat. Acad. Sci*. **2002**, *99*, 4945−4949. (e) Hoki, K.; Yamaki, M.; Koseki, S.; Fujimura, Y. *J. Chem. Phys*. **2003**, *119*, 12393−12398. (f) Hoki, K.; Yamaki, M.; Koseki, S.; Fujimura, S. *J. Chem. Phys*. **2003**, *118*, 497−504. (g) Mandl, C. P.; König, B. *Angew. Chem., Int. Ed*. **2004**, *43*, 1622−1624.

(6) (a) Arai, T.; Karatsu, T.; Misawa, H.; Kuriyama, Y.; Okamoto, H.; Hiresaki, T.; Furuuchi, H.; Zeng, H.; Sakuragi H.; Tokumaru, K. *Pure Appl. Chem*. **1988**, *60*, 989−998. (b) Waldeck, D. H. *Chem. Rev*. **1991**, *91*, 415−436. (c) Arai, T.; Tokumaru, K. *Chem. Rev*. **1993**, *93*, 23−39. (d) Görner, H.; Kuhn H. J. In *Advances in Photochemistry, Vol. 19*; Neckers, D. C.; Volman, D. H.; von Bünau, G., Eds.; Wiley: New York, 1995; pp 1−117. (e) Saltiel, J.; Sears, D. F., Jr.; Ko, D.-H.; Park, K.-M. In *CRC* Handbook of Organic Photochemistry and Photobiology; Horspool, W. M.; Song, P.-S., Eds.; CRC Press: Boca Raton, 1995; pp 3−15. (f) Arai, T. In *Organic Molecular Photochemistry*; Ramamurthy, V.; Schanze, K. S., Eds.; Marcel Dekker: New York, 1999; pp 131−167. (g) Rao, V. J. In *Organic Molecular Photochemistry*; Ramamurthy, V.; Schanze, K. S., Eds.; Marcel Dekker: New York, 1999; pp 169−209.

(7) Dewar, M. J. S.; Kohn, M. C. *J. Am. Chem. Soc*. **1972**, *94*, 2699−2704.

(8) (a) Downing, A. P.; Ollis, W. D.; Sutherland, I. O. *J. Chem. Soc. B* **1969**, 111−119. (b) Olsson, T.; Sandström, J. *Acta Chem. Scand*. **1982**, *B36*, 23−30.

(9) (a) Dreyer, J.; Klessinger, M. *J. Chem. Phys*. **1994**, *101*, 10655−10665. (b) Bearpark, M. J.; Bernardi, F.; Olivucci, M.; Robb, M. A.; Smith, B. R. *J. Am. Chem. Soc*. **1996**, *118*, 5254−5260.

(10) (a) Bergmann, E. D.; Fischer, E. *Bull. Soc. Chim. Fr*. **1950**, 1084−1091. (b) Bergmann, E. D.; Fischer, E.; Hirshberg, Y. *Bull. Soc. Chim. Fr*. **1950**, 1103−1104.

(11) Ong, B. S.; Keoshkerian, B.; Martin, T. I.; Hamer, G. K. *Can. J. Chem*. **1985**, *63*, 147−152. A solution of 40% Triton B in methanol was used, rather than 40% Triton B in pyridine, as reported in the original procedure (94% yield).

(12) Paul, G. C.; Gajewski, J. J. *Synthesis* **1997**, 524−526.

(13) (a) Bree, A.; Zwarich, R. *J. Chem. Phys*. **1968**, *51*, 903−912. (b) Sagiv, J.; Yogev, A.; Mazur, Y. *J. Am. Chem. Soc*. **1977**, *99*, 6861−6869. (c) Boo, B. H.; Choi, Y. S.; Kim, T.-S.; Kang, S. K.; Kan, Y. H.; Lee, S. Y. *J. Mol. Struct*. **1996**, *377*, 129−136.

(14) Fischer, G.; Muszkat, K. A.; Fischer, E. *J. Chem. Soc. B* **1968**, 1156−1158.

(15) Sheldrick, G. M. SHELXTL97: *Program for Structure Refinement*: University of Goettingen: Goettingen, Germany, 1997.